Published in final edited form as:
Biochemistry. 2013 May 7; 52(18): 3062–3073. doi:10.1021/bi301571v.

Methylated Nω-Hydroxy-L-arginine Analogues as Mechanistic Probes for the Second Step of the Nitric Oxide Synthase-Catalyzed Reaction†

Kristin Jansen Labby[1], **Huiying Li**[2], **Linda J. Roman**[3], **Pavel Martásek**[3,4], **Thomas L. Poulos**[2,*], and **Richard B. Silverman**[1,*]

[1]Department of Chemistry, Department of Molecular Biosciences, Chemistry of Life Processes Institute, Center for Molecular Innovation and Drug Discovery, Northwestern University, 2145 Sheridan Road, Evanston, Illinois 60208-3113

[2]Departments of Molecular Biology and Biochemistry, Chemistry, and Pharmaceutical Sciences, University of California, Irvine, Irvine, California, 92697-3900

[3]Department of Biochemistry, University of Texas Health Science Center, San Antonio, Texas 78384-7760

[4]Department of Pediatrics, First School of Medicine, Charles University, Prague, Czech Republic

Abstract

Nitric oxide synthase (NOS) catalyzes the conversion of L-arginine to L-citrulline through the intermediate N^{ω}-hydroxy-L-arginine (NHA), producing nitric oxide, an important mammalian signaling molecule. Several disease states are associated with improper regulation of nitric oxide production, making NOS a therapeutic target. The first step of the NOS reaction has been well-characterized and is presumed to proceed through a compound I heme species, analogous to the cytochrome P450 mechanism. The second step, however, is enzymatically unprecedented and is thought to occur via a ferric peroxo heme species. To gain insight into the details of this unique second step, we report here the synthesis of NHA analogues bearing guanidinium-methyl or -ethyl substitutions and their investigation as either inhibitors of or alternate substrates for NOS. Radiolabeling studies reveal that N^{ω}-methoxy-L-arginine, an alternative NOS substrate, produces citrulline, nitric oxide, and methanol. On the basis of these results we propose a mechanism for the second step of NOS catalysis in which a methylated nitric oxide species is released and is further metabolized by NOS. Crystal structures of our NHA analogues bound to nNOS have been solved, revealing the presence of an active site water molecule only in the presence of singly methylated analogues. Bulkier analogues displace this active site water molecule; a different mechanism is proposed in the absence of the water molecule. Our results provide new insight into the steric and stereochemical tolerance of the NOS active site and substrate capabilities of NOS.

†Coordinates have been deposited with the Protein Data Bank (codes: 4FVW, 4FVX, 4FVY, 4FVZ, 4FW0, and 4GQE.

*Correspondence to Prof. Richard B. Silverman at the Department of Chemistry, Agman@chem.northwestern.edu; 847-491-5653, Prof. Thomas L. Poulos, poulos@uci.edu; 949-824-7020.

PDB Accession Codes. The PDB accession codes for NHA analogues with nNOS, shown in Figures 3 and S10 are as follows: nNOS-NMOA, 4FVW; nNOS-NEOA, 4FVX; nNOS-NHMA, 4FVY; nNOS-NMMA, 4FVZ; nNOS-MHA, 4FW0; nNOS-tBOA, 4GQE.

Supporting Information Available

Supporting information is available, including: synthetic methods, substrate and inhibitor plots, ^{14}C-labeling methods, crystal structure information, MeOX and FDH reactions, HPLC-MS confirmation of NDA- and DNPH derivatives, and NMR spectra of final products. This material is available free of charge via the Internet at http://pubs.acs.org.

Nitric oxide synthases (NOSs) catalyze the oxygenation of L-arginine to L-citrulline and nitric oxide (NO) using molecular oxygen (O_2) and NADPH (Scheme 1). NO is an important signalling molecule with a wide range of biological functions.(1–3) There are three mammalian NOS isoforms. As products of distinct genes, they maintain highly conserved active sites across all three isoforms and other species. Two are constitutive isoforms, neuronal NOS (nNOS) and endothelial NOS (eNOS), which are involved in neuronal signalling and vascular regulation, respectively.(4, 5) Inducible NOS (iNOS) is expressed in macrophage cells in response to invasion of pathogens.(3) Misregulation of NO has been implicated in various disease states,(1–3) and therefore NOSs are sought-after therapuetic targets. Better understanding of the NOS mechanism will aid in the design of novel NOS inhibitors.

NOSs are homodimeric enzymes with a reductase domain that binds NADPH, FAD, and FMN, and an oxygenase domain, which contains heme and binds L-arginine and (*6R*)-5,6,7,8-tetrahydrobiopterin (H_4B). The mechanism catalyzed by NOS occurs in two distinct steps (Scheme 1). In the first step, L-arginine is monooxygenated to N^{ω}-hydroxy-L-arginine (NHA). This is proposed to occur through an oxygen rebound mechanism via the Compound I (CpdI, $Fe^{IV\bullet+}$=O) heme species, analagous to cytochrome P450 chemistry (Scheme 2).(6) H_4B provides the second electron required for oxygen activation.(7, 8) In the second step, NOS converts NHA to citrulline and NO, which requires only one electron. This step is thought to proceed through a ferric peroxo species.(9, 10) Early mechanistic proposals included the nucleophilic addition of the ferric peroxide heme species (Fe^{III}-OO^{-}) to the guanidino carbon of NHA.(11–14) Recent EPR/ENDOR cryoreduction/annealing experiments provide evidence that an active species is ferric hydroperoxide ($Fe^{III}OOH$), and in this case, the mechanism could involve a nucleophilic attack of the hydroperoxide on the guanidinium oxime.(15) The source of the proton that forms $Fe^{III}OOH$ is unknown, but it is speculated to be either an active site water molecule or the substrate itself.(14) The tetrahedral intermediate formed from addition of a ferric peroxo will then collapse, yielding citrulline and nitric oxide. In this step, H_4B also serves as a donor of the electron required for oxygen activation. It further acts as an electron acceptor when it is re-reduced either by the tetrahedral intermediate before collapse or by product NO^{-}, since overall this reaction is only a one-electron oxidation.(7) Substrate identity, and perhaps more importantly its pK_a (arginine pK_a = 12.5; NHA pK_a = 8.5),(16) are thought to dictate the formation of these different active heme species in steps one and two.

Although many experiments have been reported, details of the NOS mechanism remain elusive. During NOS turnover, the precise role of H_4B and when it is implicated, the true identity of the active heme species, and the source of protons (and how many are required) are still controversial.(17, 18) An active site water molecule has been speculated to play an important role in proton donation – either as a single proton donor or as a shuttle sequestering protons from the bulk solvent to the reaction site.(15, 16, 19) NOS crystal structures of various isoforms show a conserved, specifically oriented water molecule as part of a hydrogen bonding network that includes the substrate, active site residues, and the diatomic heme ligand (O_2 for catalysis, but NO and CO are used to form stable crystal structures).(13, 20) A second hypothesis is that the substrate itself acts as a proton donor; ENDOR and X-ray experiments show that NHA is most likely protonated in the active site.(21) Furthermore, Davydov and Hoffman's cryoreduction EPR experiments find that Fe^{III}-OOH formation is not pH dependent, suggesting the proton is sourced directly from NHA, not bulk solvent.(15)

The first NOS half-reaction closely resembles well-known cytochrome P450 hydroxylation chemistry, but the second-half reaction, the oxidation of an N^{ω}-hydroxyguanidine to a urea and NO, is enzymatically unprecedented. It is therefore poorly understood. Previously we

demonstrated that direct hydrogen atom abstraction from the O-H bond of NHA is not necessary for substrate turnover; N^{ω}-*tert*-butyloxy-L-arginine (tBOA) and N^{ω}-(3-methyl-2-butenyl)oxy-L-arginine are nitric oxide- and citrulline-producing NOS substrates.(22) To further probe the second step of the mechanism of NOS, we have synthesized and investigated a series of methylated (or ethylated) NHA analogues (Figure 1).

N^{ω}-Methoxy-L-arginine (NMOA) has been previously synthesized(23, 24) and has been explored as a prodrug inhibitor of arginase,(25) but has not been examined as a NOS substrate. N^{ω}-Methyl-L-arginine (NMA) functions as an inactivator (k_{inact} = 0.07 min^{-1}, K_I = 2.7 μM), a competitive inhibitor (K_i = 200 nM), and a slow, alternative substrate for NOS.(26) NOS converts NMA into N^{ω}-hydroxy-N^{ω}-methyl-L-arginine (NHMA), which is subsequently converted into citrulline, NO, and formaldehyde.(26) As substrates, NMA and NHMA both cause significant uncoupling of NADPH oxidation.(26) N^{δ}-Methyl-L-arginine (dMA) can be converted by NOS to N^{δ}-methyl-N^{ω}-hydroxy-L-arginine (MHA), but no further.(27, 28) dMA binds weakly to the NOS active site with a K_i of 1.4 mM.(27) N^{ω}-Methoxy-N^{ω}-methyl-L-arginine (NMMA) and N^{ω}-ethoxy-L-arginine (NEOA) have not been previously reported. We previously evaluated tBOA as a NOS substrate,(22) and here we re-examine a co-crystal structure of this compound bound in the nNOS active site. In this report, we present the synthesis, enzymatic evaluation, co-crystal structures, and novel mechanistic insights with respect to these five substrate analogues (Figure 1) as they relate to the second step of the NOS catalytic mechanism (Scheme 2).

MATERIALS AND METHODS

General Methods

All chemicals, unless otherwise noted, were obtained from Sigma Aldrich and used without further purification. Michaelis-Menten kinetics and non-linear regressions were plotted and analyzed using GraphPad Prism5.0c software. Complete procedures for the syntheses, as well as the characterization of NMOA, NEOA, NEOA, NHMA, NMMA, MHA, and [^{14}C]-NMOA, can be found in the Supporting Information.

Measuring NO Production

Murine iNOS(29) and rat nNOS(30) were expressed and purified from *E. coli* as previously described. NO production was monitored using the hemoglobin capture assay at 22 °C.(31) In addition to various final concentrations of the analogue being evaluated, assay mixtures contained 100 μM NADPH, 3 μM hemoglobin-A0 (Sigma H0267), 10 μM H_4B, in 100 mM HEPES with 10% glycerol (pH 7.5). For nNOS assays, 1 mM $CaCl_2$ and 300 U/mL CaM were added. For K_i determination, assays contained 10 μM L-arginine. Assays were initiated by addition of enzyme (approximately 100 nM final concentration), and methemoglobin formation was monitored for 1 min at 401 nm using a Shimadzu UV-1800 spectrophotometer. K_m and k_{cat} values were determined from nonlinear regressions (Michaelis-Menten). For K_i determinations, IC_{50} values were first calculated using nonlinear regressions (dose-response inhibition, four parameter variable slope). Subsequent K_i values were determined using the Cheng-Prushoff relationship $K_i = IC_{50}/(1 + [S]/K_m)$, where a K_m of 8.3 μM was used for murine iNOS.(32)

When noted, NO production was also measured with the Greiss reagent(31) using the nitrite/nitrate colormetric assay kit from Cayman Chemical (760871). Enzyme incubations contained various concentrations of the compound being evaluated, 100 nM iNOS, 100 μM NADPH, 10 μM H_4B, in 100 mM HEPES with 10% glycerol (pH 7.5). Lactate dehydrogenase was added to the reactions to oxidize excess NADPH, and then Griess

reagents were added to report nitrate. Absorbance was measured at 540 nm using a Synergy H1 Biotek plate reader.

Determination of the Spectral Binding Constant, K_S

Binding affinities for iNOS were determined using the previously described ferric difference spectral binding assay.(33) Since all compounds were type I heme-coordinating, imidazole, a type II coordinating compound, was used to initially coordinate the heme. The K_s value was then determined from displacement of the imidazole. To a 500 μL quartz cuvette was added 5 μM iNOS, 10 μM H_4B, and 100 mM HEPES (pH 7.5) to 200 μL total volume. This cuvette was scanned against a blank containing 100 mM HEPES with 10 μM H_4B. Spectra were taken from 380 to 500 nm. To determine the binding affinity of imidazole, spectra were taken after the addition of aliquots of the imidazole (0.5 to 1 mM final concentration). To assay NHA analogues, 300 μM imidazole was used, aliquots of the analogue being examined (0.1 to 1 mM final concentration) were added, and spectra were obtained for each. The total volumes added were kept below 10 μL (5%) to avoid dilution effects. Michaelis-Menton curves were determined for the imidazole as well as for each inhibitor by plotting concentration versus absorbance difference (local maximum – local minimum). Then Hanes-Wolff plots were used to determine the K_s for imidazole and the apparent K_s for the NHA analogues.(34) The K_s for imidazole with iNOS was found to be 120 – 150 μM over multiple experiments; K_s values of analogues were determined using the following equation:

$$\text{apparent } K_s = \text{actual } K_s\,(1+[\text{imidazole}]/K_{s\,\text{imidazole}}).$$

NDA Derivatization and HPLC Separation

NDA-derivatization reactions contained 25 μL of amino acid standard or sample, 25 μL of 30 mM $NaCN^{\omega}$ in 100 mM $NaB(OH)_3$ buffer pH 10, and 15 μL of 10 mM NDA in methanol. NDA reactions achieve completion nearly immediately, so all reactions were analyzed after 10 min. Phenylalanine was used as an internal standard to track complete derivatization and assure complete injection. Reactions were analyzed by reversed-phase HPLC (10 μL injection) using an Econosil C18 column with 80% 5 mM sodium acetate pH 6.0: 20% MeOH as Solvent A and 100% acetonitrile as Solvent B. A gradient from 25% B to 75% B was run over 30 min at 0.75 mL/minute. Under these conditions, NDA-derivatized amino acids had the following retention times: citrulline 4.2 min; phenylalanine 9.4 min; NHA 10.5 min; NMOA 11.7 min; NHMA 11.2 min; NMMA 12.8 min. An NDA-citrulline standard curve (R^2 = 0.995) was linear from 100 μM to 1 mM.

Measuring Substrate Uncoupling

iNOS-substrate enzyme rections (300 μL total volume in quartz cuvettes, containing 100 μM NADPH, 10 μL H_4B, 100 nM iNOS, 3 μM hemoglobin-A0, and 100 mM HEPES pH 7.5) were dually monitored at 401 nM and 340 nM for 1 min. Substrates were evaluated at the following final concentrations: 20 μM arginine, 20 μM NHA, 100 μM NMOA, and 100 μM NHMA. Reactions were initiated by the addition of iNOS. Extinction coefficents used were ε_{HbNO} = 38,000 M^{-1} cm^{-1} and ε_{NADPH} = 6.22 mM^{-1} cm^{-1}.(35)

DNPH-Derivatization Reactions

DNPH-derivatization reactions were set up by combining 20 μL of aldehyde standard or sample with 10 μL of 20 mM DNPH in 0.4 M H_2SO_4 in 10% H_2O, 90% acetonitrile. DNPH derivatization reactions proceed quickly to completion, so all reactions were injected after 10 min. All DNPH-derivatized reactions were separated by reverse-phase HPLC (10 μL injection) under the following conditions: a Phenomonex Luna C18 column was used with

water as Solvent A and acetonitrile as Solvent B. A gradient from 10% B to 90% B was run over 30 min at 1.0 mL/min. DNPH-derivatives were detected at 360 nm. Under these conditions, DNPH eluted at 12.2 min and DNPH-formaldehyde eluted at 13.3 min (DNPH-acetaldehyde 14.2 min, DNPH-acetone 14.9 min). A DNPH-formaldehyde standard curve ($R^2 = 0.995$) was linear from 100 μM to 1.5 mM.

HPLC MS Confirmation of NDA- and DNPH-derivatives

The identities of all NDA- and DNPH-derivatized products of the [^{14}C]-NMOA reactions were confirmed by liquid chromatography-mass spectrometry using an Agilent 1200 series purification system equipped with a diode array detector (SL 1315C) set to 460 (or 360) and 254 nm and an Agilent 6130A Single Quad detector using atmospheric pressure electrospray ionization (API-ES) in positive mode. A Phenomenex Gemini-NX C18 (4.6 x 50 mm, 5 μm, 100 Å) column was used with Solvent A as LCMS grade water + 0.1 % formic acid and Solvent B as LCMS grade ACN$^{\omega}$+ 0.1 % formic acid. For NDA-derivatizations, the following gradient was run at a flow rate of 1.5 mL/min: 0–7 minutes (5 – 50 % B), 7–10 minutes (100 % B). Derivatives had the following retention times: NDA-NHA 4.2 min; NDA-citrulline 6.2 min; NDA-NMOA 4.4 min; NDA-NHMA 4.4 min; NDA-NMMA; 4.6 min. For DNPH-derivatizations, the following gradient was used: at a flow rate of 1.5 mL/min, from 0–10 minutes (10 – 90 % B). DNPH-formaldehyde eluted at 3.26 minutes under these conditions.

Crystal Structure Determination

The heme domain of rat nNOS protein sample and crystals were prepared according to the procedures reported previously.(36) Fresh crystals (1–2 days old) were first passed stepwise through cryo-protectant solutions(36) and then soaked with 10 mM NHA analogues for 4–6 h at 4 °C before being mounted on nylon loops and flash cooled by plunging into liquid nitrogen. The cryogenic (100 K) X-ray diffraction data were collected remotely at various beamlines at Stanford Synchrotron Radiation Lightsource or Advanced Light Source through the data collection control software and a crystal mounting robot. Raw data frames were indexed, integrated, and scaled using HKL2000.(37) The binding of NHA analogues was detected by the initial difference Fourier maps calculated with REFMAC.(38) The analogue molecules were then modeled in COOT(39) and refined using REFMAC. Water molecules were added in REFMAC and checked through COOT. The TLS protocol(37, 40) was implemented in the later stage of refinements with each subunit as one TLS group. Finally, an additional round of TLS refinement was carried out with the coordinates of substrate analogue and the water of interest removed from the input model. The map coefficients in the output were used to produce the omit Fo – Fc electron density maps shown in Supplemental Figure S10. The refined structures were validated through the RCSB web server before deposition to the protein data bank. The crystallographic data collection and structure refinement statistics are summarized in Table 1 with PDB accession codes included.

MeOX and FDH Reactions

MeOX and FDH were obtained from Sigma Aldrich (A2404 and F8649, respectively). 10 μL of 80 U/mL MeOX in 100 mM HEPES pH 7.5 was reacted with 100 μL of sample (methanol standards, or iNOS-substrate reactions) for one hour at room temperature. MeOX reactions with methanol standards, followed by DNPH derivatization and HPLC separation produced a standard curve ($R^2 = 0.89$) with detection limit of 100 μM. [^{14}C]-NMOA-iNOS reactions incubated with MeOX were DNPH derivatized (see Methods) and analyzed by HPLC and scintillation counted. Reactions longer than one hour did not show stoichiometric turnover.

In a 20 mL glass scintillation vial the following were combined: 100 uL of [^{14}C]-NMOA-iNOS reaction, 10 μL 80 U/mL MeOX and 10 μL 80 U/mL FDH. The vial was sealed with a septum containing a suspended 1 mL plastic well. The vial was reacted for 12 hours at room temperature. Using a syringe, 200 μL of an 8 % (v/v) aqueous solution of NaOH was carefully added to the plastic well and 200 μL of a 20 % (v/v) aqueous solution of TCA was added to the multi-enzyme reaction in the bottom of the vial. The vial was further incubated at 37 °C with gentle shaking for 2 hours. The suspended reaction well was carefully separated from the vial and each were scintillation counted. Supplementary Figure S10 shows the chromatograms for those experiments.

RESULTS

Synthesis of the NHA Analogues

NMOA, NEOA, NHMA, and NMMA were synthesized through nucleophilic addition of appropriate amines to a protected ornithine thiourea (see Supplemental Scheme S1).(24, 41) MHA was synthesized by the procedure of Clement and coworkers.(42) tBOA was synthesized as previously described and was purified by HPLC.(22)

Kinetic Evaluation of NHA Analogues

NO production from iNOS and nNOS was evaluated using the hemoglobin capture assay, which monitors the absorbance increase at 401 nm as the hemoglobin-NO complex is produced.(31) Figure 2 shows Michaelis-Menten curves for NHA analogues that behave as substrates, Table 2 reports kinetic values for the compounds measured, Supplementary Figure S1 provides the individual Michaelis-Menten curves used for the determination. The mechanism is speculated to be highly conserved among NOS isoforms. In many cases we examine both isoforms, while in other experiments (such as crystal structure determination), we use only nNOS. Subtle mechanistic differences between NOS isoforms are not taken into account. Of the five NHA analogues studied, only NMOA and NHMA were found to produce NO. Overall, the substrates have a slightly greater affinity for nNOS than iNOS. Alternative substrates, NMOA and NHMA, produce NO with similar K_m values to that for NHA, but with lower k_{cat} (turnover) values; the k_{cat} for NMOA is about 4 and 7 times lower and that for NHMA is about 18 and 13 times lower with iNOS and nNOS, respectively, when compared to NHA. Kinetic trends are the same for both NOS isoforms; for nNOS and iNOS, NMOA has a weaker binding affinity for the active site (higher K_m), but greater turnover (higher k_{cat}) than NHMA. An enzyme would likely be evolutionarily optimized for its native substrate, so the lower enzyme efficencies (k_{cat}/K_m) for these analogues are expected. The absence of NO production was confirmed for NEOA, NMMA, and MHA by longer incubations with iNOS (1, 2, 6, 12, and 24 hours) using the Griess reagent.(31)

Spectral binding affinities (K_s) for iNOS were also determined (Table 2, Figures S2–S8) using the previously described spectral binding assay.(33) In this assay, imidizole, which coordinates directly to the heme iron causing a Soret shift, is first bound to NOS and then NHA analogues are titrated into the cuvette while monitoring the Soret shift as these compounds displace the imidazole (see Methods). Therefore, these values directly reflect the affinity the compound has for the active site. For the substrates, K_s values are similar to K_m values, as expected. For the compounds that are not substrates, the K_s values may rationalize why turnover cannot occur. MHA, for example, was found to have a very high K_s value, indicating its very poor binding affinity. This was confirmed upon analysis of the crystal structure (see below). NEOA and NMMA are not substrates, but have good binding affinities, so other factors must be preventing these compounds from being substrates.

Inhibition constants (K_i) with iNOS were determined for those compounds that were not substrates (Table 2, Figure S9). Slow substrates will also be competitive inhibitors, but measuring a K_i value is not meaningful since slower, alternate substrate turnover is also occurring. For the four compounds for which K_i values are meaningful (NEOA, NMMA, MHA, and tBOA), and therefore reported, these values agree with binding affinity (K_s) values. The K_i and the K_s for MHA are both very high, over 10 mM, while the K_i values for NEOA and NMMA are mid-micromolar. K_i values also indicate competition with arginine, thereby confirming that the analogues are inhibiting NOS at its active site.

We also re-evaluated tBOA, a previously reported weak NOS substrate. It has a poor binding affinity for iNOS, evidenced by its 7.4 mM K_i value and 2.7 mM K_m value. tBOA has the slowest k_{cat}, about one-third the rate of NHMA, the slowest of our NHA analogues for iNOS.

The NHA analogues were also evaluated as time-dependent inactivators of iNOS. In all cases, NOS activity was fully restored by addition of L-arginine to pre-incubations of each compound with iNOS under turnover conditions, indicating that time-dependent inactivation was not occurring (Figure S9C).

Citrulline Production

For substrates NMOA and NHMA, the amino acid product was confirmed to be solely citrulline (chromatographs are shown in Supplementary Figure S13). This was done by naphthalene-2,3-dicarboxyaldehyde-(NDA)-derivatization of the products of NOS (both iNOS and nNOS were used and performed in at least triplicate) reactions with subsequent HPLC separation and spectral detection at 460 nm (see Methods). An authentic standard of N^{ω}-cyanoornithine (CN-Orn) was prepared to confirm its absence in all of the analogue-NOS reactions.

NADPH Consumption and NO Production

The rates of production of NO and consumption of NADPH were compared for all substrates (Table 3) with iNOS. NO production was measured using the hemoglobin capture assay, monitoring methemoglobin formation at 401 nm, while simultaneously measuring the conversion of NADPH to $NADP^+$ at 340 nm. Table 3 shows that arginine and NHA consume approximately 1.5 and 0.5 equivalents, respectively, of NADPH for each NO molecule released. NMOA and NHMA, however, consume many more equivalents of NADPH (8 and 15, respectively) than NO is produced. This result is consistent with the slower k_{cat} values (Table 2) for these two analogues when compared to that of NHA; NMOA and NHMA are not efficent substrates for NOS.

Determination of the One-Carbon Metabolite of NMOA

NOS turnover of NMOA produces citrulline and NO, leaving the methyl of the N^{ω}-methoxyl group unaccounted for. To address this issue, N^{ω}-[^{14}C]-methoxy-L-arginine ([^{14}C]-NMOA) was synthesized using the chemistry shown in Supplementary Scheme S1, (24, 41) with the exception that [^{14}C]-methoxylamine (34 mCi/mmol) was used as the amine added to the activated thiourea (**2**, Scheme S1).

iNOS reactions with [^{14}C]-NMOA, NMOA, NHA, or substrate-free were 1) analyzed by NDA-derivatization and HPLC separation to quantify amino acids, 2) analyzed by 2,4-dinitrophenyl hydrazine (DNPH)-derivatization and HPLC separation to identify aldehydes and ketones, and 3) allowed to react with methanol oxidase and/or formate dehydrogenase to convert methanol into formaldehyde and formate and to convert formate into bicarbonate, respectively (Scheme 3). Before HPLC analysis, reactions were filtered through a 10,000

MWC filter. Filters were found to contain no [^{14}C], indicating that covalent modification of the enzyme is not occurring.

NDA-derivatization of the [^{14}C]-NMOA-iNOS reaction was separated by HPLC and scintillation counted (see Supplementary Figure S10). These spectra show that the only [^{14}C] species to elute, in addition to [^{14}C]-NMOA, is located in the early fractions (2–4 minutes), suggesting that this metabolite is highly polar. We hypothesize that this is a one-carbon metabolite from the [^{14}C]-NMOA-iNOS reaction. DNPH was next used to detect aldehydes and ketones from the iNOS reactions in search of formaldehyde as a potential one-carbon biproduct of [^{14}C]-NMOA-NOS metabolism. With an excess of DNPH no significant amount of ^{14}C eluted with DNPH-formaldehyde standards, indicating that the one-carbon metabolite from these reactions is not formaldehyde.

Numerous attempts at detecting methanol directly by chromatography or mass spectrometry were unsuccessful, which excluded experiments run in isotopic water or oxygen. Consequently, enzymatic conversion was employed to convert any methanol produced to formaldehyde, then to formic acid, then to carbon dioxide, as depicted in Scheme 3. Methanol oxidase (MeOX) converts methanol to formaldehyde and H_2O_2 with a K_m of approximately 2 mM (depending on the O_2 concentration), but also catalyzes the conversion of formaldehyde to formate with a K_m of 2.5 mM.(43) Following reaction with MeOX, [^{14}C]-NMOA-iNOS reactions produced small amounts of [^{14}C]-DNPH-formaldehyde, but stoichiometrically less than the amount of citrulline produced by the same reactions in the absence of MeOX, because of the conversion of some of the produced formaldehyde to formate by MeOX. To better quantify the methanol formation in the iNOS-catalyzed reaction, [^{14}C]-NMOA was incubated with a mixture of iNOS, MeOX, *and* formate dehydrogenase (FDH); FDH converts the formate produced in the MeOX reaction to bicarbonate, which, after acidification, produces carbon dioxide, which can be trapped in base, allowing for quantitative detection of all of the [^{14}C] metabolites as DNPH-formaldehyde and CO_2. Experiments repeated with MeOX but with FDH omitted did not produce [^{14}C]-CO_2, confirming the identity of the one-carbon metabolite of the [^{14}C]-NMOA-iNOS reaction as [^{14}C]-methanol exclusively.

Crystal Structures of the Substrate Analogues

Crystal structures of substrate analogues bound to rat nNOS oxygenase domain were obtained (Figure 3 and omit electron densities in Figure S11). Similar to NHA and arginine, all analogues retain the four hydrogen bonds conserved for an L-amino acid moiety: AA-COO^- to Tyr588-OH; AA-COO^- to Asp597-COO^- ; AA-NH_3^+ to Glu592-COO^-; and AA-NH_3^+ to heme propionate A. The planarity of the guanidino group is, more or less, maintained for all compounds but MHA. This planarity allows the two guanidino nitrogens, N^{δ} and $N^{\omega'}$, to hydrogen bond to Glu592. These key interactions place the guanidino head over the heme for potential catalysis. However, with MHA the presence of an N^{δ}-methyl destroys the planarity of guanidine, resulting in only one hydrogen bond from the $N^{\omega'}$ nitrogen to Glu592. The close distance (~ 3.9 Å) from the extra N^{δ}-methyl to heme could be sterically preventing O_2 from binding to the heme iron, thus preventing turnover. Steric blockage of productive oxygen binding was hypothesized to be the reason that arginine and NHA analogues bearing a C5 methyl substitution at the *pro-R* position are not substrates.(19) The electron density for MHA is the poorest among the five analogue structures, which reflects unfavorable interactions between the distorted guanidino group of MHA and the NOS active site and is consistent with the poor binding affinity determined for this compound (see Table 2).

Similar to NHA, the N^{ω}-OH of NHMA and MHA forms a weak hydrogen bond to the backbone nitrogen of Gly586 (Figure 3). Any substituent on this hydroxyl group would

eliminate this hydrogen bond by either dragging the oxygen atom away from Gly586 as in NEOA, totally swinging away as in NMMA, or being blocked by a methyl group as in NMOA (Figure 3). The orientation and bulkiness of this substituted hydroxyl will, in turn, influence whether or not an active site water molecule can bind next to the analogue. The active site water usually hydrogen bonds to the substrate N^{ω} atom. This hydrogen bonding interaction is maintained in NHMA, and is at least partially retained in MHA and NMOA via the oxygen atom from the analogue. In MHA the water molecule is not fully occupied because of the closeness of the hydroxyl group; while in NMOA the methyl of the methoxyl moiety adopts two conformations, the predominant conformation, shown in Figure 3B, allows for a partially occupied water molecule that shares the same space with the methyl group in its minor conformation (Figure S11A). However, in NEOA and NMMA either an ethyl or a methyl group, respectively, occupies the space of the active site water. In the nitric oxide ferrous complex of nNOS, this same water molecule is within hydrogen-bonding distance of the O atom of NO, and thus is in an ideal position to serve as a proton donor.(20)

We also have obtained a crystal structure of tBOA in the active site of nNOS (see Figure S12). There is no water molecule present in the active site in this co-crystal structure. The *tert*-butyl group is apparently too bulky to fit in the site and is, therefore, disordered; the three *tert*-butyl methyl groups exchange their positions but are populated more in the space that a water molecule normally occupies. Therefore, there is no active site water molecule present even though this compound is a weak substrate.

DISCUSSION

The products of NOS turnover with the various NHA analogues was investigated. Citrulline is the only amino acid product formed from NMOA and NHMA. In addition to citrulline, NOS produces CN-Orn when NHA is the substrate and when H_2O_2 is used in place of NADPH.(44) It is speculated that citrulline is the product of native NOS-NHA chemistry (through the ferric peroxo intermediate), while CN-Orn is the product of non-native NOS-NHA chemistry, when NOS is forced to go through CpdI.(10) Since citrulline is the only amino acid product of NMOA and NHMA, this suggests NOS is performing native chemistry through Fe^{III}-OO^{-}/Fe^{III}-OOH, not through CpdI, on these substrates.

There is significantly higher consumption of NADPH per NO released for substrates NMOA and NHMA (8 and 15 equiv, respectively) in comparison to L-arginine and NHA (1.5 and 0.5 equiv, respectively). These ratios were measured at substrate concentrations approximately equal to their K_m values. Uncoupling of substrate turnover from electron consumption happens when superoxide ($O_2^{\bullet -}$) is released from the ferric superoxide complex ($Fe^{III}OO^{\bullet}$; see Scheme 2) before substrate modification. This unproductive consumption of electrons by NOS occurs at subsaturating concentrations of L-arginine or H_4B.(6, 35) Uncoupling also occurs in the presence of alternate substrates such as homoarginine(45) or inactivators such as N^5-(1-iminooethyl)-L-ornithine,(46) suggesting substrate identity affects the feasibility of oxidation. *B. subtilis* NOS Trp66 (the Trp residue that hydrogen bonds to H_4B) mutants also show uncoupling.(47) This demonstrates the importance of the entire NOS enzyme structure in implementing efficiently coupled substrate turnover and that even seemingly small, single residue, changes can largely affect enzymatic outcomes. Both substrates, NMOA and NHMA, show some uncoupling during turnover, which means NADPH reducing equivalents may be used for the production of other products, such as superoxide, rather than NO (Table 3). A highly coupled system requires precise proton transfer steps, and therefore those substrates that are uncoupled, very likely, perturb the local proton transfer mechanism. It should be noted that substrate oxidation is a multi-step process and that alternative substrates may potentially affect other steps, for example, electron transfer from the reductase. Furthermore, the consistency

between low k_{cat} values (Table 2) and higher uncoupling for NMOA and NHMA suggests that oxidation of these alternative subsrtates represents only 5 to 10% of iNOS catalysis. The decrease in k_{cat} (approximately 5 and 10% the k_{cat} of NHA) could be the result of this dramatic degree of uncoupling.

The one-carbon metabolite of [^{14}C]-NMOA was found to be methanol. This result differs from the one-carbon metabolite determined to be present in NOS-NHMA reactions; Olken and Marletta found that NHMA produces formaldehyde, first going through NHA as an intermediate.(26). The higher uncoupling (Table 3) of NHMA compared to NMOA is consistent with the fact that NHMA processing requires an additional oxidation step to yield the observed formaldehyde. This suggests that different substrates are metabolized by NOS through different mechanisms.

We have previously reported(22) that both N^{ω}-*tert*-butyloxy-L-arginine and N^{ω}-(3-methyl-2-butenyl)oxy-L-arginine are NOS substrates; therefore, a direct hydrogen atom abstraction from the N$^{\omega}$-OH hydroxyl does not appear to be required in the second step of the NOS reaction for these two alternative substrates. It, therefore, may seem surprising that NHMA is a NOS substrate since NHMA lacks the N$^{\omega}$-H proton. In light of this, we propose that at least one of the two protons, either the N$^{\omega}$-H or the N$^{\omega}$O-H proton, is necessary for turnover. The positions of these protons are seemingly interchangeable because of the conformational isomers that exist, and either may be functioning as a proton source during oxygen activation (see Figure 4A). Density functional theory calculations suggest that both are comparable in energy for hydrogen atom donation.(21) Crystal structures typically reflect the most stable binding conformation, but do not reveal other possible conformations that may exist under the dynamic conditions of an enzyme active site. By comparison of the crystal structures for the three substrates, along with their turnover rates, we hypothesize that deprotonation at the N$^{\omega}$-H is favored on the basis of its physical proximity to the heme-iron and on the slower k_{cat} for NHMA than NMOA (Table 2). While even the native substrate (NHA) may go through many pathways, this suggests that the N$^{\omega}$-H, positioned down towards the heme-iron (Figures 4B and 4C), is more easily removed, but that the N$^{\omega}$O-H, positioned farther away from the heme-iron (Figures 4B and 4D), can also serve as a viable proton source, but less efficiently. The substrate might rotate around the C-N$^{\omega}$ bond in order for the N$^{\omega}$ O-H to be aligned for deprotonation, but since this is not the conformation depicted in the crystal structure, it is likely not the most energetically favorable conformation. The fact that NMMA, a compound in which both the N$^{\omega}$-H and the N$^{\omega}$ O-H protons are replaced with methyl groups, has good binding affinity for the NOS active sites but is not a NOS substrate, is consistent with our hypothesis that the presence of at least one N$^{\omega}$ proton is essential for turnover.

Previous ENDOR and X-ray experiments, as well as DFT calculations, show that NHA is most likely protonated in the active site.(21) The existence of a water molecule next to the guanidino group of the substrate could play a role in maintaining its protonated state, thus affecting the rate of catalysis. On the basis of the substrate activities of NMOA and NHMA, and the lack of activity with NMMA, we propose a possible mechanism for the reaction of NOS with NHA and NMOA (Scheme 4). The turnover and one carbon metabolite of NHMA has been previously examined in detail.(26) As shown in Scheme 4, the ferric superoxide heme species is activated upon receiving an electron from H_4B. The resulting ferric peroxide species is then protonated by the substrate to form the reactive ferric hydroperoxide species. On the basis of experimental evidence supporting $Fe^{III}OOH$ as the active species, (15) and our results suggesting the necessity of the active site proton, we hypothesize that $Fe^{III}OOH$ needs to be formed to create the proper “push-pull” dynamics and electronics for the reaction to occur. The ferric hydroperoxide then undergoes attack on the electrophilic guanidinium carbon. Driven by the formation of citrulline, this tetrahedral intermediate

collapses, producing a protonated or methylated nitric oxide species, which is subsequently processed, aided via appropriate proton transfers by the active site water molecule. A heme-NO complex forms, which donates an electron back to the radical cation of H_4B to produce H_4B, NO, and ferric heme. This proposed mechanism invokes the active site water in the processing of the released NO-containing product; however, additional roles, such as other proton transfers, structural stability, or pK_a maintenance, are also possible.

Because both NMOA and NHMA are NOS substrates, but NMMA is not, it is reasonable to conclude that NOS can process a singly-methylated NO species, but not a doubly-methylated species. However, although the proton is necessary, it is not sufficient, as NEOA has the N^{ω}-H proton available, but is not a substrate. This can be accounted for by considering two mechanistic pathways: 1) in a nucleophilic pathway, as shown in Scheme 4, an $N^{\omega}O$-ethyl species may be too sterically hindered to undergo reaction, while methyl-$N^{\omega}O$ and $N^{\omega}O$-methyl species are more reactive and can be processed by NOS, or 2) in an electrophilic cleavage of the $N^{\omega}O$-R bond it would be expected that none of the small alkyl-substituted analogues are likely to be cleaved because of the high energy of the resulting cation. N^{ω}-*tert*-Butyloxy-L-arginine and N^{ω}-(3-methyl-2-butenyl)oxy-L-arginine(22), however, are substrates, which argues in favor of the second mechanism and against the first. According to the second mechanism, the stability of the resulting cations (*tert*-butyl and dimethylallyl, respectively) might suggest that these compounds should be excellent substrates, but they are only weak substrates. (22) The crystal structures of NEOA (Figure 3E) and tBOA (Supplemenary Figure S12) show that there is no active site water molecule bound; the bulky hydrophobic substituents apparently displace it. However, whereas NEOA is not a substrate, tBOA is a substrate, suggesting that the water molecule may not be essential for activity, and, perhaps more importantly, that there is likely more than one mechanism by which substrates can be turned over. Perhaps, substrates with larger substituents that displace the water molecule but can form stabilized carbocations are metabolized through a mechanism that does not require a water molecule, a mechanism in which electron transfer from the H_4B to ferric superoxide occurs initially followed by ferric peroxide attack on the substrate (Scheme 5). Because of the stability of the resulting carbocation, spontaneous breakdown of the tetrahedral intermediate gives citrulline, HNO, and ferrous oxo radical. Abstraction of a hydrogen atom from HNO by $Fe^{II}O^{\bullet}$ with loss of water produces the heme-NO complex. As in Scheme 4, the radical cation of H_4B accepts an electron to give NO and ferric heme. In the case of NEOA, the water molecule is displaced but because an ethyl cation is not sufficiently stable, breakdown of the second intermediate does not occur, and the equilbrium favors substrate.

In the unique case of MHA bound to nNOS, an active site water, at least partially, exists, and both N^{ω} protons are present, but this compound is not a substrate. In the crystal structure (Figure 3F) the N^{δ}-methyl distorts the planarity of the guanidino group, thereby weakening its crucial interactions with Glu592, which contributes to its poor binding affinity. The close positioning of this N^{δ}-methyl to the heme-iron (~3.9 Å) could prevent productive binding of molecular oxygen.

The role of the active site water in the second step of NOS catalysis is still quite controversial. Martin and coworkers cleverly examined C5-methylated arginine and NHA analogues, finding that N^{ω}-hydroxy-(5*S*)-methyl-L-arginine is a NOS substrate while (5*S*)-methyl-L-arginine is not.(19) They speculated that both analogues bearing a (5*S*)-methyl substituent displace the active site water molecule. On the basis of their modeling results, they suggested that the active site water is required for the first step of NOS catalysis, but is not required for the second step. The NHA analogue crystal structures presented here (Figure 2) show that, when present, the active site water molecule does not bind near C5, but interacts with N^{ω} near Ser585, and MHA, which has an N^{δ}-methyl substituent, still binds

with an active site water molecule (Figure 3F). On the basis of our crystal structures, it is possible that (5*S*)-methyl compounds also would allow active site water binding; further structural data is needed to confirm this hypothesis. However, as supported by the example of tBOA, this water molecule cannot be deemed essential for catalysis with all NHA analogues; our results suggest it does play a role in the turnover of NHA, NMOA, and NHMA.

Our findings suggest that substrate identity, especially its steric bulkiness, dictates the ability of a water molecule to bind in the active site; if the water is involved in the predominant turnover pathway, its binding could determine the ability of NOS to catalyze a reaction on a substrate and determine the rate of catalysis. A caveat to this hypothesis arises because our crystal structures do not contain a heme-oxo species; substrates would be repositioned when O_2 binds and/or the O_2 ligand must bend in a different direction than we have observed in the NO complexes of nNOS and eNOS. When NO coordinates to the heme iron in nNOS, the substrate, L-arginine, must move about 0.7 Å.(20) The substrates under investigation in this study are larger, causing greater steric restriction for O_2 binding and hence must move to enable O_2 to bind. Even so, there still should be sufficient room for the “catalytic” water to remain in place and provide a potential proton source for catalysis in the cases of NMOA and NHMA.

Compared to their substrate-promiscuous cytochrome P450 relatives, NOSs are very specific enzymes because of their small, highly conserved active sites. An intricate set of hydrogen bond interactions holds substrates in the active site. The research described here demonstrates that NOS can metabolize several different substrates and may proceed through different mechanisms during metabolism of these various substrates.

In summary, we demonstrate that NOS can metabolize NHA analogues having a methyl substituted for either the N^{ω}-H proton (NHMA) or the N^{ω}-OH hydroxyl proton (NMOA), but not both (NMMA), and this is consistent with the importance of either the N^{ω}-H proton or the N^{ω}-OH proton in catalysis. Crystal structures reveal the presence of an active site water molecule that could also serve as a proton donor during substrate turnover, but *tert*-butoxy-L-arginine acts as a substrate, even though the *tert*-butyl group displaces the active site water, as shown in the crystal structure. We propose potential, alternative pathways (Schemes 4 and 5) consistent with our findings for these analogues as NOS substrates. Our crystal structures demonstrate that substrate identity dictates the presence or absence of the active site water molecule, but this does not always dictate substrate turnover. As a unique and complex enzyme, NOS not only is able to achieve two different oxygenation chemistries (step one and step two) within its active site, but is also flexible enough to oxidize various substituted NHA analogues, possibly by more than one mechanism.

Supplementary Material

Refer to Web version on PubMed Central for supplementary material.

Acknowledgments

Funding

This work was funded by National Institutes of Health, Grants GM049725 to RBS, and GM057353 to TLP. We thank Dr. Bettie Sue Siler Masters (NIH grant GM52419, with whose laboratory P.M. and L.J.R. are affiliated). B.S.S.M. also acknowledges the Welch Foundation for a Robert A. Welch Distinguished Professorship in Chemistry (AQ0012). P.M. is supported by grant 0021620849 from MSMT of the Czech Republic. Support for KJL was provided by Reach for the Stars, a GK-12 program supported by the National Science Foundation under grant DGE-0948017.

We thank the SSRL and ALS beamline staff for their support during remote X-ray diffraction data collection. We thank Dr. Jinwen Huang for synthesizing the NEOA.

Abbreviations

NOS	nitric oxide synthase
NO	nitric oxide
NHA	N^{ω}-hydroxy-L-arginine
nNOS	neuronal nitric oxide synthase
eNOS	endothelial nitric oxide synthase
iNOS	inducible nitric oxide synthase
H_4B	(*6R*)-5,6,7,8-tetrahydrobiopterin
CYP450	cytochrome P450
CpdI	compound I
tBOA	N^{ω}-*tert*-butyloxy-L-arginine
NMOA	N^{ω}-methoxy-L-arginine
NEOA	N^{ω}-ethoxy-L-arginine
NHMA	N^{ω}-hydroxy-N^{ω}-methyl-L-arginine
MHA	N^{δ}-methyl- N^{ω}-hydroxy-L-arginine
NMMA	N^{ω}-methoxy-N^{ω}-methyl-L-arginine
δMA	N^{δ}-methyl-L-arginine
[^{14}C]-NMOA	N^{ω}-[^{14}C]-methoxy-L-arginine
CN-Orn	N^{δ}-cyanoornithine
NDA	naphthalene-2,3-dicarboxyaldehyde
DNPH	2,4-dinitrophenyl hydrazine
MeOX	methanol oxidase
FDH	formate dehydrogenase

References

1. Griffith OW, Stuehr DJ. Nitric oxide synthases: properties and catalytic mechanism. Annu Rev Physiol. 1995; 57:707–736. [PubMed: 7539994]
2. Calabrese V, Mancuso C, Calvani M, Rizzarelli E, Butterfield DA, Stella AMG. Nitric oxide in the central nervous system: neuroprotection versus neurotoxicity. Nat Rev Neurosci. 2007; 8:766–775. [PubMed: 17882254]
3. Alderton WK, Cooper CE, Knowles RG. Nitric oxide synthases: structure, function and inhibition. Biochem J. 2001; 357:593–615. [PubMed: 11463332]
4. Zhou L, Zhu D-Y. Neuronal nitric oxide synthase: Structure, subcellular localization, regulation, and clinical implications. Nitric Oxide. 2009; 20:223–230. [PubMed: 19298861]
5. Förstermann U, Pollock JS, Schmidt HH, Heller M, Murad F. Calmodulin-dependent endothelium-derived relaxing factor/nitric oxide synthase activity is present in the particulate and cytosolic fractions of bovine aortic endothelial cells. Proc Natl Acad Sci USA. 1991; 88:1788–1792. [PubMed: 1705708]
6. Gorren ACF, Mayer B. Nitric-oxide synthase: a cytochrome P450 family foster child. Biochim Biophys Acta. 2007; 1770:432–445. [PubMed: 17014963]

7. Stuehr DJ, Wei C-C, Wang Z, Hille R. Exploring the redox reactions between heme and tetrahydrobiopterin in the nitric oxide synthases. Dalton Trans. 2005:3427–3435. [PubMed: 16234921]
8. Stoll S, NejatyJahromy Y, Woodward JJ, Ozarowski A, Marletta MA, Britt RD. Nitric oxide synthase stabilizes the tetrahydrobiopterin cofactor radical by controlling its protonation state. J Am Chem Soc. 2010; 132:11812–11823. [PubMed: 20669954]
9. Hurshman AR, Marletta MA. Reactions catalyzed by the heme domain of inducible nitric oxide synthase: evidence for the involvement of tetrahydrobiopterin in electron transfer. Biochemistry. 2002; 41:3439–3456. [PubMed: 11876653]
10. Woodward JJ, Chang MM, Martin NI, Marletta MA. The second step of the nitric oxide synthase reaction: evidence for ferric-peroxo as the active oxidant. J Am Chem Soc. 2009; 131:297–305. [PubMed: 19128180]
11. Feldman PL, Griffith OW, Stuehr DJ. The surprising life of nitric-oxide. Chem Eng News. 1993; 71:26–38.
12. Korth HG, Sustmann R, Thater C, Butler AR, Ingold KU. On the mechanism of the nitric oxide synthase-catalyzed conversion of N^{ω} -hydroxyl-L-arginine to citrulline and nitric oxide. J Biol Chem. 1994; 269:17776–17779. [PubMed: 7517932]
13. Pant K, Crane BR. Nitrosyl-heme structures of *Bacillus subtilis* nitric oxide synthase have implications for understanding substrate oxidation. Biochemistry. 2006; 45:2537–2544. [PubMed: 16489746]
14. Crane BR, Sudhamsu J, Patel BA. Bacterial nitric oxide synthases. Annu Rev Biochem. 2010; 79:445–470. [PubMed: 20370423]
15. Davydov R, Sudhamsu J, Lees NS, Crane BR, Hoffman BM. EPR and ENDOR characterization of the reactive intermediates in the generation of NO by cryoreduced oxy-nitric oxide synthase from *Geobacillus stearothermophilus*. J Am Chem Soc. 2009; 131:14493–14507. [PubMed: 19754116]
16. Giroud C, Moreau MM, Mattioli TA, Balland V, Boucher JL, Xu-Li Y, Stuehr DJ, Santolini J. Role of arginine guanidinium moiety in nitric-oxide synthase mechanism of oxygen activation. J Biol Chem. 2010; 285:7233–7245. [PubMed: 19951943]
17. Santolini J. The molecular mechanism of mammalian NO-synthases: a story of electrons and protons. J Inorg Biochem. 2011; 105:127–141. [PubMed: 21194610]
18. Daff S. NO synthase: structures and mechanisms. Nitric Oxide. 2010; 23:1–11. [PubMed: 20303412]
19. Martin NI, Woodward JJ, Winter MB, Beeson WT, Marletta MA. Design and synthesis of C5 methylated L-arginine analogues as active site probes for nitric oxide synthase. J Am Chem Soc. 2007; 129:12563–12570. [PubMed: 17892291]
20. Li H, Igarashi J, Jamal J, Yang W, Poulos TL. Structural studies of constitutive nitric oxide synthases with diatomic ligands bound. J Biol Inorg Chem. 2006; 11:753–768. [PubMed: 16804678]
21. Tantillo DJ, Fukuto JM, Hoffman BM, Silverman RB, Houk KN. Theoretical studies on $N^{\omega G}$-hydroxy-l-arginine and derived radicals: Implications for the mechanism of nitric oxide synthase. J Am Chem Soc. 2000; 122:536–537.
22. Huang H, Hah JM, Silverman RB. Mechanism of nitric oxide synthase. Evidence that direct hydrogen atom abstraction from the OH bond of N^{G}-hydroxyarginine is not relevant to the mechanism. J Am Chem Soc. 2001; 123:2674–2676. [PubMed: 11456942]
23. Komori Y, Wallace GC, Fukuto JM. Inhibition of purified nitric oxide synthase from rat cerebellum and macrophage by L-arginine analogs. Arch Biochem Biophys. 1994; 315:213–218. [PubMed: 7527206]
24. Schade D, Kotthaus J, Clement B. Efficient synthesis of optically pure N^{ω}-alkylated l-arginines. Synthesis. 2008; 2008:2391–2397.
25. Schade D, Kotthaus J, Klein N, Kotthaus J, Clement B. Prodrug design for the potent cardiovascular agent N^{ω}-hydroxy-L-arginine (NOHA): synthetic approaches and physicochemical characterization. Org Biomol Chem. 2011; 9:5249–5259. [PubMed: 21625725]

26. Olken NM, Marletta MA. N^G-Methyl-L-arginine functions as an alternate substrate and mechanism-based inhibitor of nitric oxide synthase. Biochemistry. 1993; 32:9677–9685. [PubMed: 7690590]
27. Luzzi SD, Marletta MA. L-arginine analogs as alternate substrates for nitric oxide synthase. Bioorg Med Chem Lett. 2005; 15:3934–3941. [PubMed: 15993059]
28. Kotthaus J, Schade D, Töpker-Lehmann K, Beitz E, Clement B. N(delta)-Methylated L-arginine derivatives and their effects on the nitric oxide generating system. Bioorg Med Chem. 2008; 16:2305–2312. [PubMed: 18083522]
29. Hevel JM, White KA, Marletta MA. Purification of the inducible murine macrophage nitric oxide syntase: Identification as a falvoprotein. J Biol Chem. 1991; 266:22789–22791. [PubMed: 1720773]
30. Roman LJ, Sheta EA, Martásek P, Gross SS, Liu Q, Masters BSS. High-level expression of functional rat neuronal nitric oxide synthase in Escherichia coli. Proc Natl Acad Sci USA. 1995; 92:8428–8432. [PubMed: 7545302]
31. Hevel JM, Marletta MA. Nitric-oxide synthase assays. Methods Enzymol. 1994; 233:250–258. [PubMed: 7516999]
32. Cheng YC, Prusoff WH. Relationship between the inhibition constant (Ki) and the concentration of inhibitor which causes 50 per cent inhibition (I50) of an enzymatic reaction. Biochem Pharmacol. 1973; 22:3099–3108. [PubMed: 4202581]
33. Martell JD, Li H, Doukov T, Martásek P, Roman LJ, Soltis M, Poulos TL, Silverman RB. Heme-coordinating inhibitors of neuronal nitric oxide synthase. Iron-thioether coordination is stabilized by hydrophobic contacts without increased inhibitor potency. J Am Chem Soc. 2010; 132:798–806. [PubMed: 20014790]
34. Silverman, RB. The Organic Chemistry of Enzyme-Catalyzed Reactions. 2. Academic Press; San Diego: 2002. p. 563-596.
35. Adak S, Wang Q, Stuehr DJ. Arginine conversion to nitroxide by tetrahydrobiopterin-free neuronal nitric-oxide synthase. Implications for mechanism. J Biol Chem. 2000; 275:33554–33561. [PubMed: 10945985]
36. Li H, Shimizu H, Flinspach ML, Jamal J, Yang W, Xian M, Cai T, Wen EZ, Jia Q, Wang PG, Poulos TL. The novel binding mode of N-alkyl-N′-hydroxyguanidine to neuronal nitric oxide synthase provides mechanistic insights into NO biosynthesis. Biochemistry. 2002; 41:13868–13875. [PubMed: 12437343]
37. Otwinowski Z, Minor W. Processing of X-ray diffraction data collected in oscillation mode. Methods Enzymol. 1997; 276:307–326.
38. Murshudov GN, Vagin AA, Dodson EJ. Refinement of macromolecular structures by the maximum-likelihood method. Acta Crystallogr. 1997; 53:240–255.
39. Emsley P, Lohkamp B, Scott WG. Features and development of Coot. Acta Crystallogr. 2010; D66:486–501.
40. Winn MD, Isupov MN, Murshudov GN. Use of TLS parameters to model anisotropic displacements in macromolecular refinement. Acta Crystallogr. 2001; D57:122–133.
41. Martin NI, Woodward JJ, Marletta MA. NG-hydroxyguanidines from primary amines. Org Lett. 2006; 8:4035–4038. [PubMed: 16928067]
42. Schade D, Töpker-Lehmann K, Kotthaus J, Clement B. Synthetic approaches to N(delta)-methylated L-arginine, N(omega)-hydroxy-L-arginine, L-citrulline, and N(delta)-cyano-L-ornithine. J Org Chem. 2008; 73:1025–1030. [PubMed: 18179234]
43. van der Klei IJ, Bystrykh LV, Harder W. Alcohol oxidase from *Hansenula polymorpha* CBS 4732. Methods Enzymol. 1990; 188:420–427. [PubMed: 2280715]
44. Clague MJ, Wishnok JS, Marletta MA. Formation of N^{δ}-cyanoornithine from N^G-hydroxy-L-arginine and hydrogen peroxide by neuronal nitric oxide synthase: implications for mechanism. Biochemistry. 1997; 36:14465–14473. [PubMed: 9398165]
45. Moali C, Boucher J-L, Sari M-A, Stuehr DJ, Mansuy D. Substrate specificity of NO synthases: detailed comparison of L-arginine, homo-L-arginine, their N^{ω}-hydroxy derivatives, and N^{ω}-hydroxynor-L-arginine. Biochemistry. 1998; 37:10453–10460. [PubMed: 9671515]

46. Fast W, Nikolic D, van Breemen RB, Silverman RB. Mechanistic studies of the inactivation of inducible nitric oxide synthase by N5-(1-Iminoethyl)-l-ornithine (L-NIO). J Am Chem Soc. 1999; 121:903–916.

47. Brunel A, Wilson A, Henry L, Dorlet P, Santolini J. The proximal hydrogen bond network modulates bacillus subtilis nitric-oxide synthase electronic and structural properties. J Biol Chem. 2011; 286:11997–12005. [PubMed: 21310962]

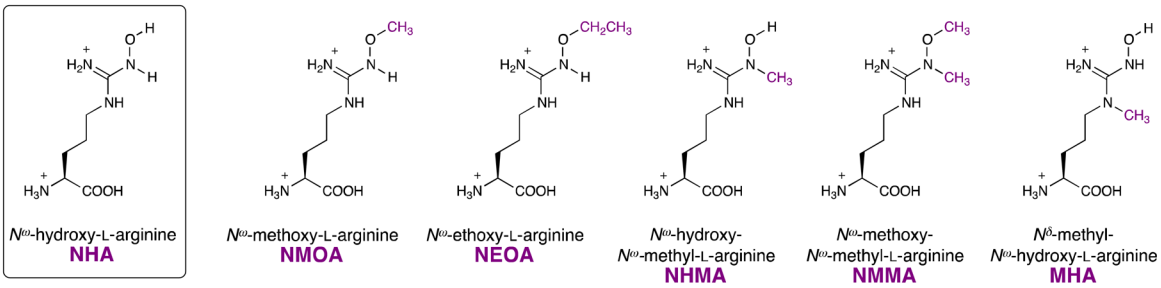

Figure 1.
NHA substrate analogues

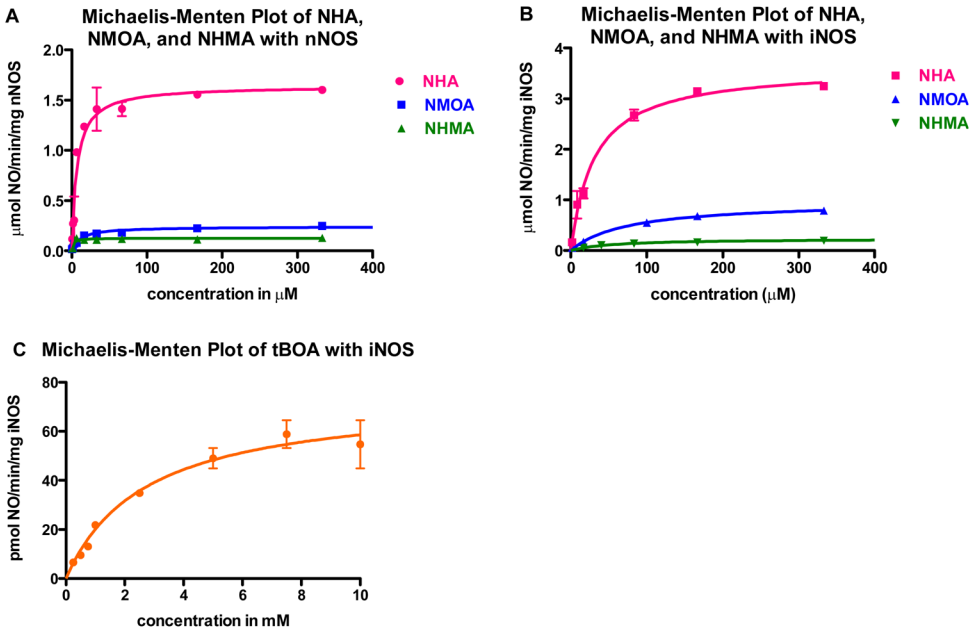

Figure 2.

Michaelis-Menten curves of NHA, NMOA, and NHMA with (A) nNOS and (B) iNOS. (C) Michaelis-Menten curve of tBOA with iNOS, note the different units along both axes. The corresponding Michaelis-Menten values are reported in Table 2.

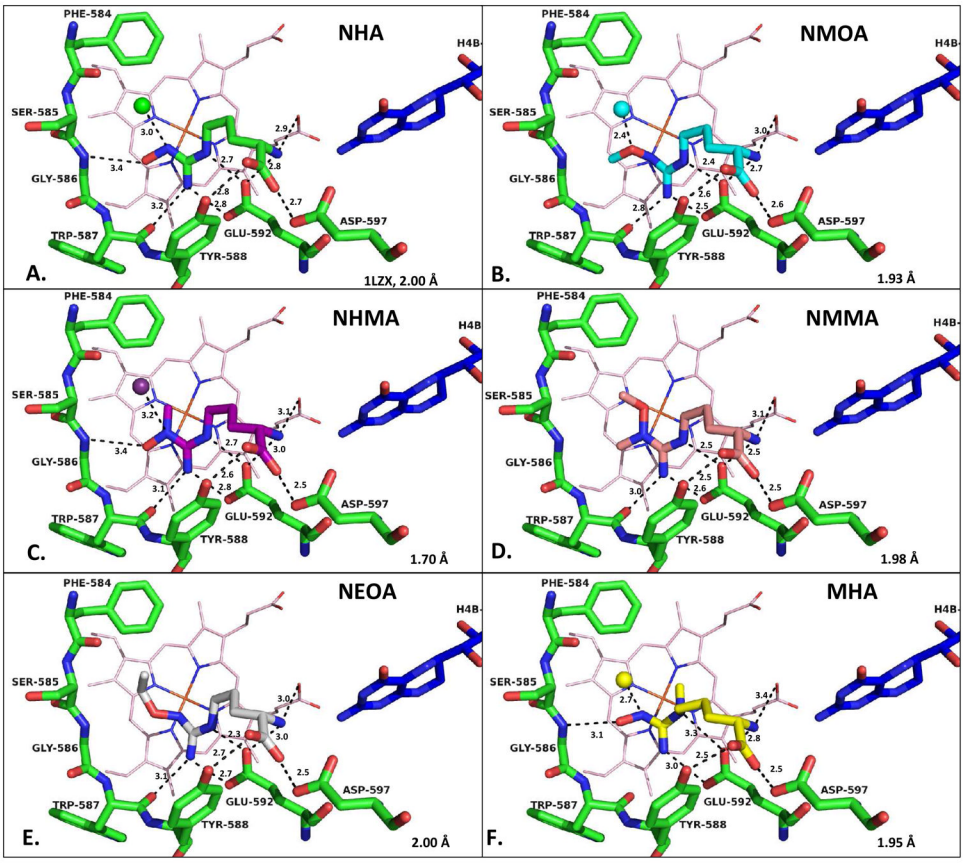

Figure 3.

Crystal structures of analogues complexed with nNOS. Heme is shown in light pink and H_4B in dark blue; nNOS active site residues are in green; active site water is shown as a sphere. **(A)** NHA (green, PDB 1LZX) **(B)** NMOA (cyan) which was modeled with the methyl group in two alternate positions but with only major one shown. **(C)** NHMA (magenta) **(D)** NMMA (peach) **(E)** NEOA (grey) **(F)** MHA (yellow), which showed poorer density quality indicating partial disordering. Hydrogen bonding interactions are depicted by black dashed lines; distances are reported in Å. See Figure S12 for crystal structure of tBOA.

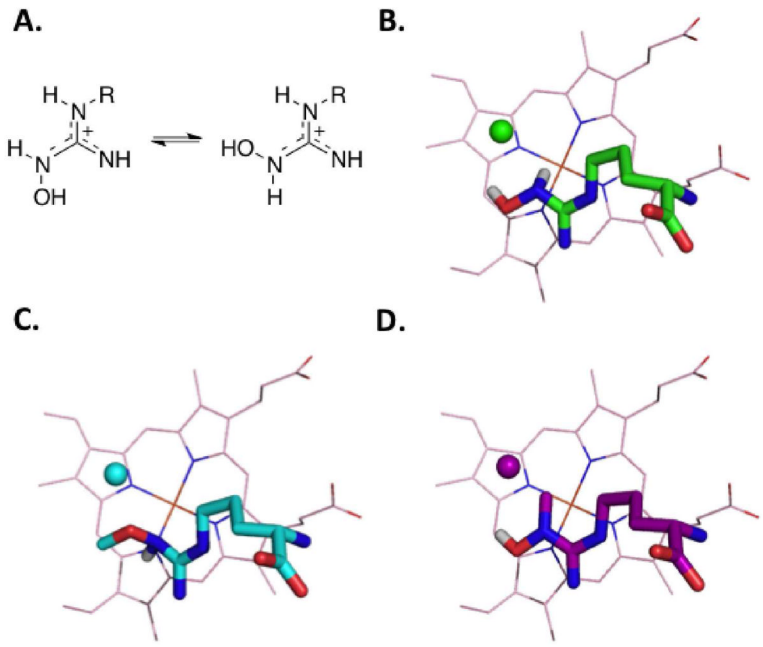

Figure 4.

(A) Conformational isomers of NHA analogues. **(B)** Crystal structure of NHA (green) with N^{ω} -H and N^{ω} -OH protons (white) rendered. **(C)** Crystal structure of NMOA (cyan) with N^{ω} -H proton (white) rendered. The methyl of the methoxyl group occupies two alternate positions, but only one is shown here. **(D)** Crystal structure of NHMA (magenta) with N^{ω} -OH proton (white) rendered. In all panels heme (light pink) is shown as lines; NHA and analogues are shown as sticks and active site water molecules as spheres. Rendered protons are white; nitrogens atoms are blue; oxygen atoms are red; carbon atom colors are specified for each substrate.

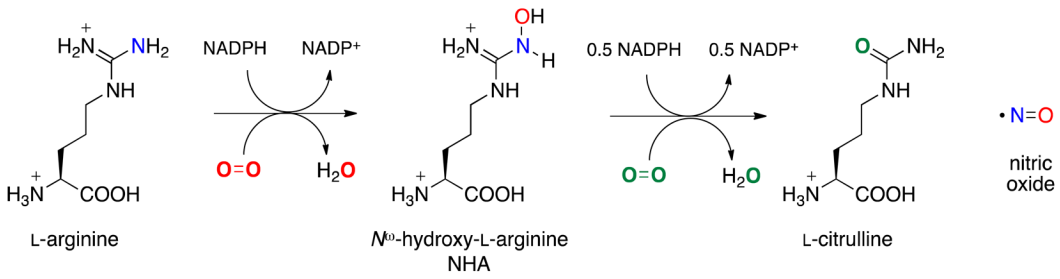

Scheme 1.
Reaction catalyzed by NOS

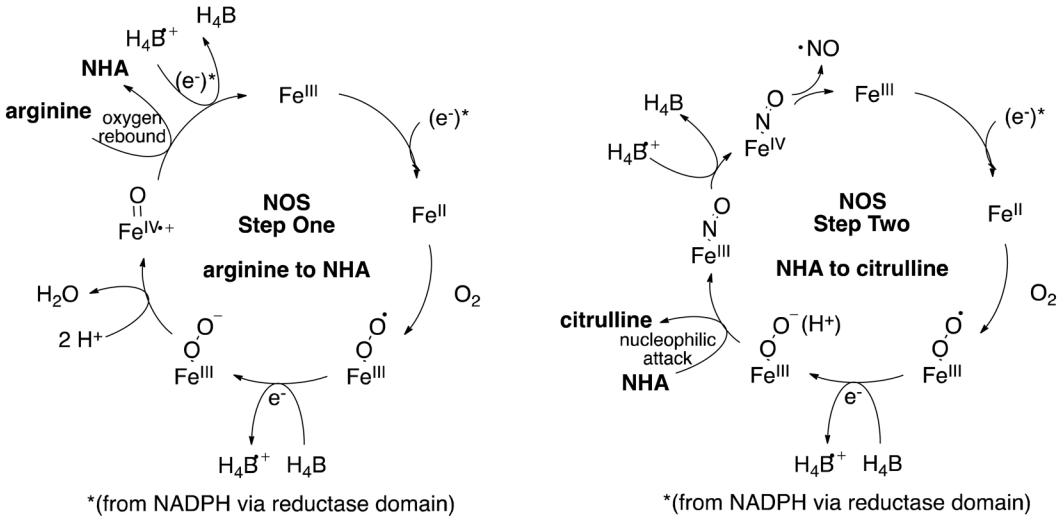

Scheme 2.
Proposed NOS mechanisms for steps one and two

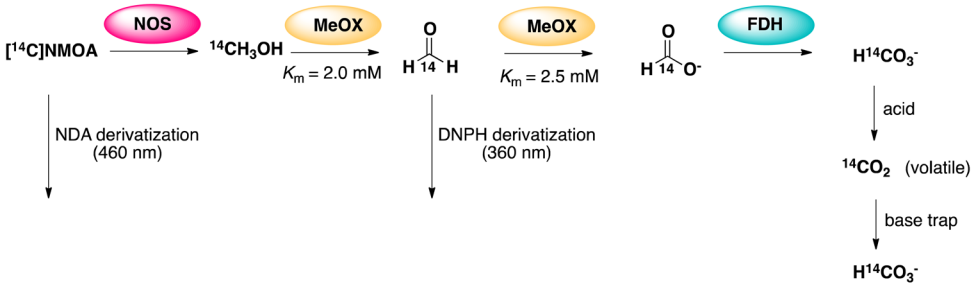

Scheme 3.

Flowchart of enzyme reactions and detection methods used in determination of the one-carbon metabolite of NMOA

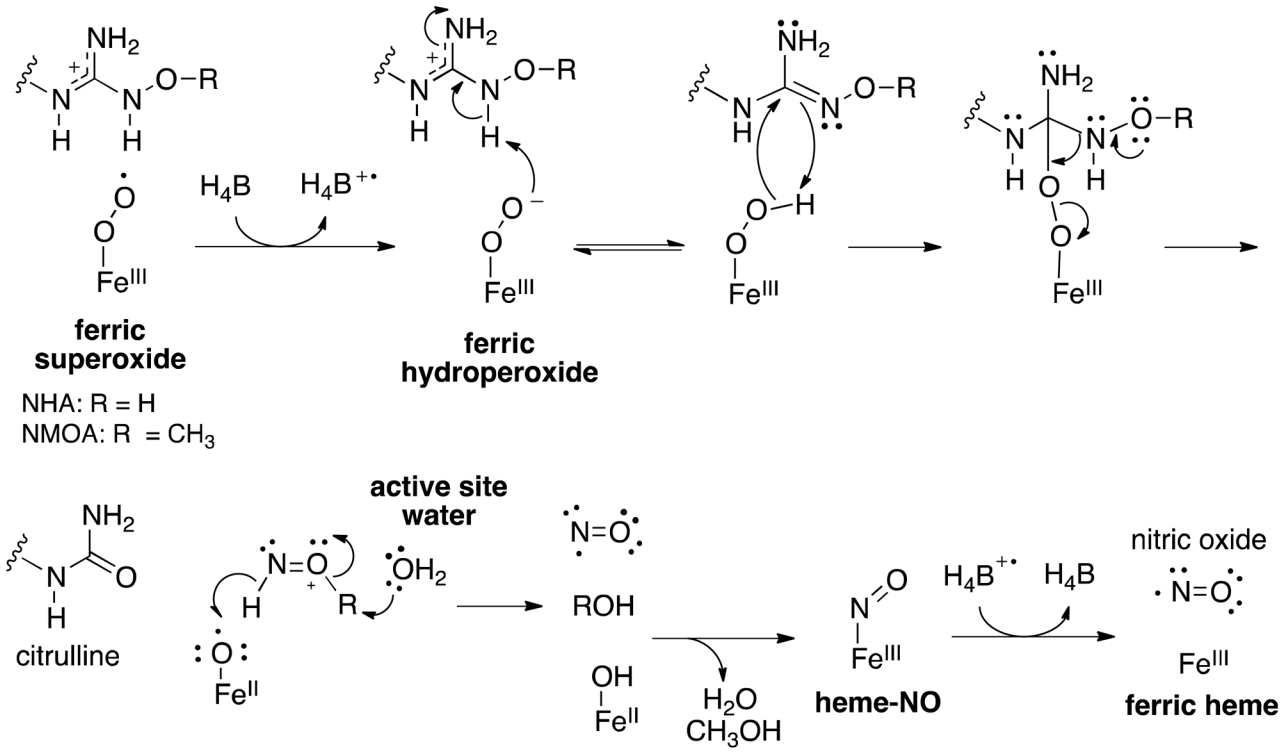

Scheme 4.
NOS turnover of NHA and NMOA.

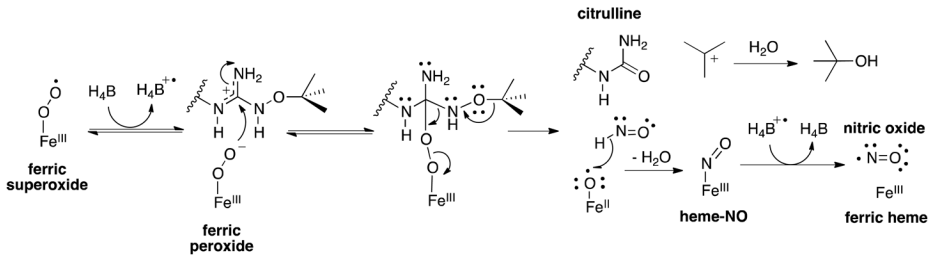

Scheme 5.
Pathway by which tBOA could be acting as a substrate despite the lack of an active site water molecule

Table 1

Crystallographic data collection and refinement statistics

Data set[a]	nNOS-NMOA	nNOS-NEOA	nNOS-NHMA	nNOS-NMMA	nNOS-MHA	nNOS-tBOA
Data collection						
PDB code	4FVW	4FVX	4FVY	4FVZ	4FW0	4GQE
Space group	$P2_12_12_1$	$P2_12_12_1$	$P2_12_12_1$	$P2_12_12_1$	$P2_12_12_1$	$P2_12_12_1$
Cell dimensions						
a	52.1	52.0	51.9	51.9	52.1	52.0
b	111.0	111.3	110.9	110.8	111.3	111.1
c (Å)	165.3	165.1	164.5	164.5	164.1	164.3
Resolution (Å)	1.80 (1.83-1.80)	2.00 (2.03-2.00)	1.70 (1.73-1.70)	2.00 (2.03-2.00)	1.95 (1.98-1.95)	1.78 (1.81 -1.78)
R_{sym} or R_{merge}	0.077 (0.626)	0.071 (0.588)	0.055 (0.443)	0.075 (0.636)	0.064 (0.662)	0.057 (0.746)
$I / \sigma I$	29.9 (1.8)	19.7 (1.7)	31.8 (2.0)	23.3 (1.9)	24.3 (2.0)	31.6 (2.3)
No. unique reflections	88,431	65,282	102,661	65,397	70,555	88,147
Completeness (%)	99.6 (99.9)	99.6 (97.8)	97.5 (99.2)	99.4 (99.9)	99.6 (99.9)	99.4 (98.7)
Redundancy	4.2 (3.6)	4.0 (3.6)	5.0 (4.6)	3.8 (3.8)	4.0 (4.0)	4.5 (3.8)
Refinement						
Resolution (Å)	1.81	2.00	1.70	2.00	1.95	1.80
No. reflections used	83,967	61,988	97,474	61,954	66,998	83,676
R_{work}/R_{free} [b]	0.181/0.218	0.181/0.221	0.184/0.212	0.202/0.248	0.194/0.232	0.189/0.222
Mean B value ($Å^2$)	48.03	47.98	36.52	52.98	43.26	46.80
No. atoms						
Protein	6687	6659	6679	6667	6655	6662
Ligand/ion	171	165	157	160	167	153
Water	374	388	419	262	322	380
R.m.s. deviations						
Bond lengths (Å)	0.013	0.013	0.012	0.015	0.013	0.013
Bond angles (deg)	2.019	1.424	1.303	1.522	1.352	2.051

[a] See Figure 1 for nomenclature and chemical formulae of NHA analogues.

[b] R_{free} was calculated with the 5% of reflections set aside throughout the refinement. The set of reflections for the R_{free} calculation were kept the same for all data sets according to those used in the data of the starting model (1OM4).

Table 2

Kinetic values determined for NHA analogues[a]

	NHA		NMOA		NHMA		NEOA	NMMA	MHA	tBOA[c]
	iNOS	**nNOS**	**iNOS**	**nNOS**	**iNOS**	**nNOS**	**iNOS**	**iNOS**	**iNOS**	**iNOS**
K_m (μM)	22 ± 5	5.7±2.1	88 ± 8	11 ± 2	34 ± 6	2.0 ± 0.4	-	-	-	2.7 ± 0.8 mM
k_{cat} (min^{-1})	16 ± 2	13 ± 4	4.7±1.3	1.8 ±0.5	0.9±0.5	1.0 ± 0.2	-	-	-	0.3 ± 0.1
k_{cat}/K_m (μM min^{-1})	0.5	2.8	0.05	0.16	0.03	0.03	-	-	-	0.11
K_s (μM)	29 ± 4	-	122 ±20	-	34 ± 4	-	120±13	70 ± 5	>10mM	-
K_i (μM)[b]	n/a		n/a		n/a		26 ± 3	28 ± 3	>10mM	7.4 ± 4.5 mM

[a] See Supplementary Information for Michaelis-Menten plots (Figure S1) and inhibition curves and difference spectra (Figures S2–9).

[b] All compounds were also evaluated as inactivators, but none was found to cause time-dependent inhibition (see Supplementary Information Figure S9).

[c] The k_{cat} value differs from that previously reported;(22) the same enzyme concentration was used here for all of the compounds, which is lower than that used in the earlier publication for tBOA, so that all data in this table could be meaningfully compared.

Table 3

Uncoupling of NO production from NADPH consumption

Substrate:	arginine	NHA	NMOA	NHMA
NADPH:NO[a]	1.7 ± 0.2	0.7 ± 0.3	8.0 ± 1.5	15.0 ± 2.7

[a]Ratios are expressed as moles of NADPH consumed per mole of NO formed with iNOS, averaged over five or more experiments.